

Jennifer Gill  
Dwayne Arola

Department of Mechanical Engineering,  
University of Maryland Baltimore County,  
Baltimore, MD 21250

Ashraf F. Fouad  
Department of Endodontics,  
Prosthodontics and Operative Dentistry,  
University of Maryland,  
Baltimore, MD 21201

Liang Zhu<sup>1</sup>  
Associate Professor  
Department of Mechanical Engineering,  
University of Maryland Baltimore County,  
Baltimore, MD 21250  
e-mail: zliang@umbc.edu

# Design of Laser Treatment Protocols for Bacterial Disinfection in Root Canals Using Theoretical Modeling and MicroCT Imaging

*Theoretical simulations of temperature elevations in root dentin are performed to evaluate, how heating protocols affect the efficacy of using erbium, chromium; yttrium, scandium, gallium, garnet (Er,Cr:YSGG) pulsed lasers for bacterial disinfection during root canal treatments. The theoretical models are generated based on microcomputer tomography (microCT) scans of extracted human teeth. Heat transfer simulations are performed using the Pennes bioheat equation to determine temperature distributions in tooth roots and surrounding tissue during 500 mW pulsed Er,Cr:YSGG laser irradiation on the root canal for eradicating bacteria. The study not only determines the heat penetration within the deep dentin but also assesses potential thermal damage to the surrounding tissues. Thermal damage is assumed to occur when the tissue is subject to a temperature above at least 47°C for a minimum duration of 10 s. Treatment protocols are identified for three representative tooth root sizes that are capable of maintaining elevated temperatures in deep dentin necessary to eradicate bacteria, while minimizing potential for collateral thermal tissue damage at the outer root surfaces. We believe that the study not only provides realistic laser heating protocols for various tooth root geometries but also demonstrates utility of theoretical simulations for designing individualized treatments in the future. [DOI: 10.1115/1.4006479]*

## Introduction

More than 15 million root canal treatment procedures are performed annually in the United States [1]. Root canal bacteria, particularly Gram-positive facultative anaerobes, seem to be remarkably resistant to local antimicrobial agents often used in root canal therapy. In fact, persistent cultivable bacteria are found in more than 40% cases [2–5]. Moreover, the success rate of treatment in cases with preoperative infections is significantly lower than in cases without infections, necessitating research on more effective root canal disinfecting protocols [6–9]. In addition to traditional approaches, intracanal heating using a laser catheter has the potential to eradicate residual bacteria in deep root dentin. However, a carefully designed heating protocol is needed to achieve a desired thermal dosage that preserves sensitive surrounding tissues of the tooth root.

Typically, the root canal system is irrigated with 0.5–5% sodium hypochlorite solution, and much of the infected hard tissue lining the canal is eliminated by mechanical instrumentation. Once this process is complete, a canal medicament, such as calcium hydroxide is applied directly to the canal walls. The medicament mostly eradicates bacteria with which it comes in direct contact. The effectiveness of calcium hydroxide, even when mixed with chlorhexidine has been called into question. Another potential reason for failure of root canal disinfection with irrigants is the difficulty in distributing the irrigants in the extremely narrow or curved regions of root canals in sufficient quantities based on instrumental and visual limitations [10]. Again, the irrigant must make direct physical contact with the bacteria in sufficient concentration for eradication. Bacterial colonies remaining in the root canal can reproduce, and may communicate with the periapical tissues despite root fillings, thus, leading to persistent infections and failure of the treatment

[11,12]. It has been reported that bacteria penetrate up to 800  $\mu\text{m}$  from the root canal surface in root dentin [4,13–15]. One study of postoperative patients concluded that the root canal procedures were successful in 68–80% of patients one year after treatment [16]. The largest factor affecting success rates is the inability to reach the apical infection with irrigant paste [17].

In dentistry, laser is typically used for soft and hard tissue ablation [18]. Due to the limitations of conventional antibacterial methods, the application of heat has been proposed for bacterial disinfection of the root dentin [19,20]. Unlike traditional disinfection methods, heat delivered by irradiation of the root canal is capable of fully penetrating the dentin tubules via conduction. The Er,Cr:YSGG laser [21–25] is of particular interest because the majority of its absorption is superficial. The absorption coefficient of the Er,Cr:YSGG laser is equal to approximately  $10^4 \text{ cm}^{-1}$  [26,27], which means that the light penetrates only 1  $\mu\text{m}$  into a dental material, making it best utilized for its thermal conductive properties and allowing it to be modeled as a heat flux for theoretical purposes. When used at a frequency of 20 Hz with pulse duration of 200  $\mu\text{s}$ , this laser has been shown to be particularly capable of bacterial elimination, as it promises a reduction in bacterial regrowth by an order of magnitude when compared with traditional treatment techniques [19]. Studies have demonstrated a 0.2% bacterial regrowth rate after laser treatment, compared to the 2.0% regrowth rate associated with conventional irrigant methods [19]. One reason contributing to this difference is the use of heat. In addition to these benefits, the optical fiber tips of the lasers have diameters as small as 200  $\mu\text{m}$ , which makes them capable of reaching the curved and narrow spaces close to the root apex, after preparing the canal to a size 20 file. If significant levels of disinfection could be achieved with lasers, this modality would be useful in future dental disinfection protocols.

In order for laser irradiation to be clinically accepted as a root canal disinfection method, a number of parameters must be optimized, including the level and duration of heating required to eradicate bacteria without damage to the adjacent tissues. A prior theoretical study [25] attempted to evaluate the resulting temperature field in tooth dentin under various heating protocols used in

<sup>1</sup>Corresponding author.

Contributed by the Heat Transfer Division of ASME for publication in the JOURNAL OF THERMAL SCIENCE AND ENGINEERING APPLICATIONS. Manuscript received August 29, 2011; final manuscript received March 19, 2012; published online July 23, 2012. Assoc. Editor: Lisa X. Xu.

clinical studies. This previous simulation illustrated, why some of the treatment protocols using low laser power levels and/or wet laser did not completely eliminate bacteria in root dentin in the *in vitro* experiment [19]. Though that study identified a heating duration to avoid collateral thermal tissue damage, it was based on a very simplified geometric model previously used in the *in vitro* clinical experiment [19]. The simplified model of a cylindrical ring structure incorporated assumptions in the tooth and canal geometry that limit the accuracy of the previous theoretical analyses. To our knowledge, there has been no theoretical study on the dentin temperature distribution arising from thermal treatment based on realistic tooth root geometry, including an assessment of temperature elevations at the cementum, periodontal ligament, and the surrounding bone.

In this study, we focus on how tooth geometry affects temperature elevations in root dentin. Heat transfer simulations are performed using the Pennes bioheat equation [28] to understand the heat distribution in root dentin during 500 mW Er,Cr:YSGG laser irradiation for bacterial disinfection. Theoretical models are generated based on microCT scans of extracted human teeth. The study not only determines the heat penetration within the deep dentin but also assesses potential thermal damage to the surrounding tissue structure. Realistic laser treatment protocols are identified that are capable of maintaining the required elevated temperature within deep dentin necessary to eradicate bacteria, while simultaneously minimizing collateral thermal tissue damage. The balance between these two factors is evaluated in the study.

## Theoretical Modeling

**Geometry Modeling Based on MicroCT Imaging of Extracted Human Teeth.** In this study, the tooth structure is established as a two-dimensional axis-symmetric model based on microCT imaging of extracted human teeth. Seven extracted single-root human teeth consisting of incisors and canines were provided by dentists in the School of Dentistry at the University of Maryland, Baltimore, according to a protocol approved by the Institutional Review Board from the University of Maryland Baltimore County. An access preparation was performed, and then the canals were prepared using standard K-files. The teeth were all kept in individual test tubes, submerged in distilled water and stored in a refrigerator in the laboratory. Prior to scanning using a microCT imaging system (Skyscan 1172, Microphotonics, PA), each tooth was thoroughly rinsed with distilled water to remove debris. These teeth were then dried with compressed air, and mounted inside a low density support structure to ensure maximum stability during the scan. The pixel size in each image was selected as 17.2  $\mu\text{m}$  (medium scan), and each image file contains  $2000 \times 1048$  pixels. Since the teeth have an aspect ratio of 3 or more, we used a set up called “oversized scan,” which combines multiple scans of individual segments. The rotation rate was set to be 0.4 deg at six

increments. Lastly, the filter was chosen as an aluminum copper filter to produce an image with the best contrast. The scans took an average of 6h for each tooth. Following completion of the scans, the NRecon<sup>®</sup> software package provided by the company was used in conjunction with the six primary computer servers to reconstruct each specimen. Using the CTAn<sup>®</sup> analysis software package, the reconstruction files allow generations of 3D tooth models or cross-sectional images of the teeth.

Although it would be ideal to import the 3D tooth model to a commercial software for heat transfer simulation, it was not feasible due to limitations of the computational memory and a large number of irregularities in the geometry not admissible to the commercial software. In this study, we model the tooth structure as a two-dimensional axis-symmetric model as a compromise. The 2D model captures the important geometrical variations pertaining to the tooth dentin structure without detrimental loss of detail. Figure 1 gives the reconstructed cross sections of the seven teeth. Based on the figure, it is clear that Tooth A (17.54 mm in root canal length) is the longest of the seven provided specimens, and Tooth D (11.65 mm in root canal length) is the shortest. The degree of brightness shown in the longitudinal-sectional images is indicative of varying densities, and thereby attenuation coefficients. The bright area surrounding the crown of the tooth is the enamel, shown most prevalent in Tooth A and Tooth C. Tooth E and Tooth D have a notably brighter material residing on the enamel surface; this is a composite filling material. Prior to obtaining the seven teeth from our collaborators at the Dental School of the University of Maryland, Baltimore, some teeth underwent a typical root canal procedure. Therefore, filling material may remain inside the root canal, and it shows as a brighter region within the root canal in the microCT images of the teeth. When these longitudinal-sectional images were used to model the geometry, these regions were excluded from the root canal models because they are not a portion of the natural tooth geometry. The region comprised of dentin in each tooth appears as a homogeneous material. The dentin tubules, with diameters of 1–2  $\mu\text{m}$ , are not visible since the pixel size was set to 17  $\mu\text{m}$ . In this study, heat transfer simulations are performed on Tooth A (the largest), Tooth F (the middle), and Tooth D (the smallest).

**Mathematical Formulation of the Heat Transfer Model.** The roots of the three teeth of interest, the largest, the middle, and the smallest, are modeled as two-dimensional axis-symmetric geometries (Fig. 2). Each geometry is imported into Comsol<sup>®</sup> as an axis-symmetric model and embedded in a section of tissue to mimic realistic conditions inside the mouth. Both the tissue and the tooth model are transformed into solid entities using the “coerce to solid” function in Comsol<sup>®</sup>. The longitudinal-sectional plane of the model is shown in Fig. 3, where the tooth root is embedded in the tissue block. The tissue block is selected large enough so that the prescribed 37 °C boundary condition on the tissue surface far away from the root canal surface is reasonable.

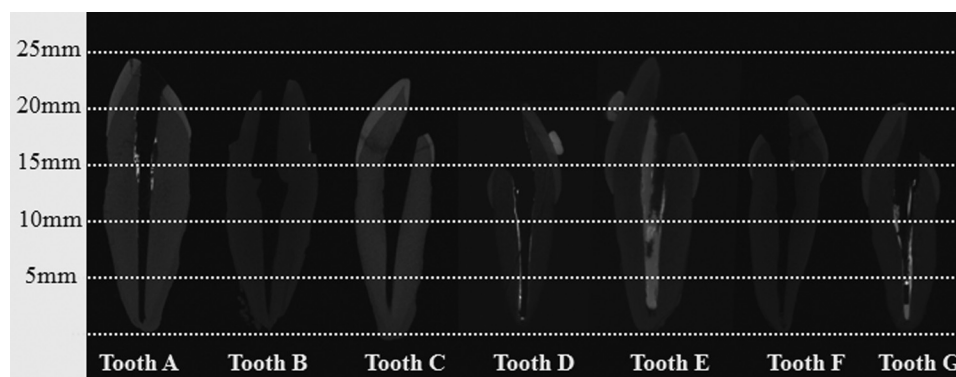


Fig. 1 Seven longitudinal-sectional images of extracted human teeth from the microCT scans

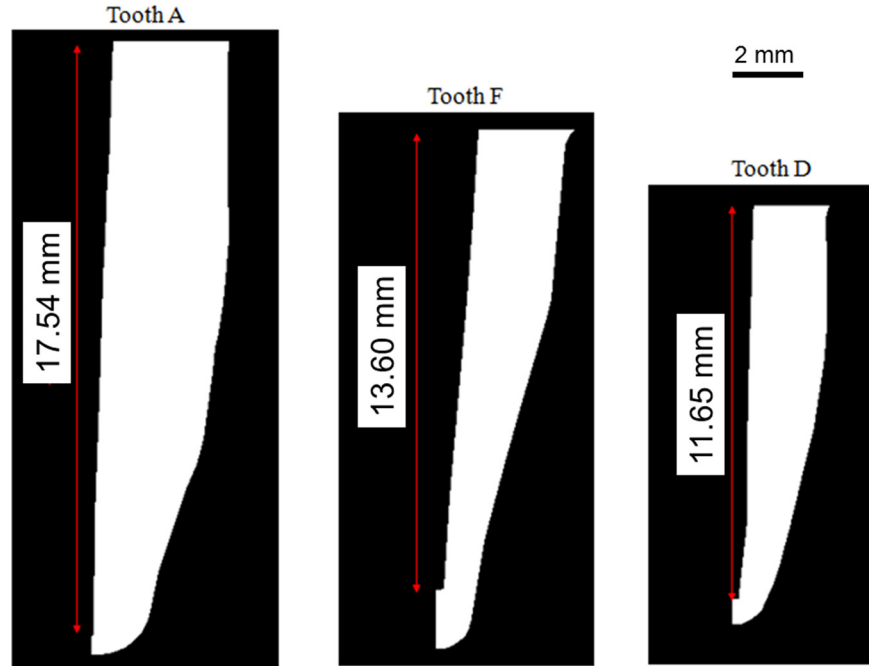


Fig. 2 Root geometries of the largest, the middle, and the smallest tooth roots to be imported to the COMSOL<sup>®</sup> software package

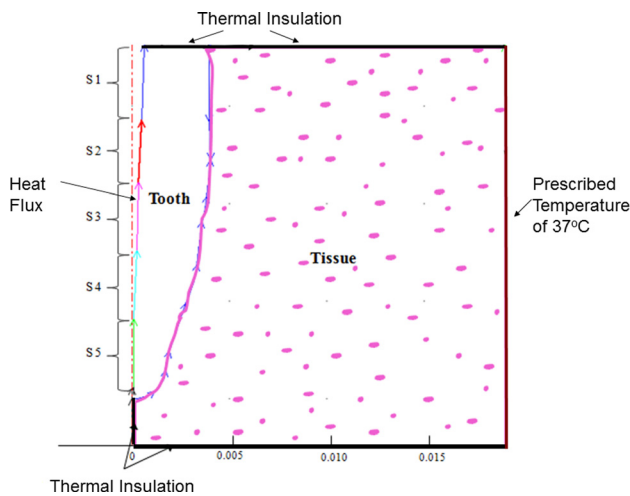


Fig. 3 The two-dimensional axis-symmetric heat transfer model of the tooth, where the root of the tooth is embedded in a tissue block

We use the Pennes bioheat equation [28] to simulate the heat transport in the tissue as a result of laser treatment. Neglecting metabolic heat generation, one can write the governing equation for temperature  $T$  as

$$\rho C \frac{\partial T_{root,tissue}}{\partial t} = k_{root,tissue} \nabla^2 T_{root,tissue} + \omega \rho_{blood} C_{blood} (37 - T_{root,tissue}) \quad (1)$$

where  $k$  is the thermal conductivity,  $\rho$  is the density,  $C$  is the specific heat, and  $\omega$  is the local blood perfusion rate. The thermal effect of the blood perfusion in the surrounding tissue is modeled as a heat source term with a strength proportional to the local blood perfusion rate, and the temperature difference between the body temperature (37 °C) and the local tissue temperature. Table 1 lists the thermal properties used in the simulation based on previous studies [29–31]. In root dentin, the blood perfusion rate is zero;

Table 1 Thermal properties used in the model

	$k$ (W/mK)	$\rho$ (kg/m <sup>3</sup> )	$C$ (J/kgK)	$\omega$ (ml/min · 100g)/(1/s)
Root	0.57	2140	1400	0.0/0.0
Tissue	1.16	1500	2300	1.8/0.0002

while, in the surrounding bony tissue it is 1.8 ml/100 g/min [30]. The initial condition is 37 °C in the entire domain. Boundary conditions are indicated in Fig. 3.

Temperature elevations in the tooth root and surrounding tissues are induced by a laser irradiance incident on the root canal surface. In this study, the laser is a commercially available Er,Cr:YSGG laser (YSGG Waterlase MD<sup>TM</sup>, Biolase Technology, Irvine, CA), pulsing with a duration of 200  $\mu$ s and a repetition rate of 20 pulses per second (20 Hz). This is the same laser used in previous clinical studies [19]. The end-firing design of the laser catheter only allows a limited emission range of approximately 1–2 mm in the axial direction. In this study, we divide the root canal surface into five segments with equal lengths in the axial direction, as shown in Fig. 3. Consistent with the current treatment practice [19], we propose that the laser tip is traversed in the canal in a cervical-apical and apical-cervical direction, while the tip stays at individual segments for specified time durations. Due to the long wavelength of the Er,Cr:YSGG laser and a large absorption coefficient of 10<sup>4</sup> cm<sup>-1</sup> in hard tissue [26,27], we assume that the laser wave will not penetrate into the tooth root. Consequently, the incident laser is modeled as a uniform heat flux incident on the canal segment when the laser tip emits radiation to that segment. Because the Er,Cr:YSGG laser is pulsed, the heat flux is modeled as a step function, as provided in the following equation:

$$q''(t) = \{q_i'' \text{ during a pulse; } 0 \text{ otherwise}\} \quad (2)$$

where  $q''$  is the heat flux function and  $q_i''$  is the heat flux during a pulse and is calculated using the following expression:

$$q_i'' = Q/A_i = E/(f * t_p * A_i), \quad i = 1, 2, 3, 4, 5 \quad (3)$$

where  $A_i$  is the root canal surface area on which the laser is incident and  $Q$  (watts) is the laser power during each pulse, which depends on the laser frequency  $f$  (Hz), pulse duration  $t_p$ (s), and laser power setting  $E$  of the laser (W). The incident surface area varies with each segment, and in this case is modeled as smooth cylindrical walls of varying diameter. The calculated laser power  $Q$  is 125 W, when the laser power setting  $E$  is 500 mW based on previous in vitro experiments and theoretical simulations [19,25]. Based on the measured root canal geometry using the microCT images, the diameter of the root canal varies from approximately 200  $\mu\text{m}$  at the apex to 2500  $\mu\text{m}$  at the root cervix. This yields a heat flux on individual canal segments from  $10^6$  to  $10^7$  W/m<sup>2</sup>.

A unique finite element model was generated for both the tissue and tooth root of each model. This resulted in meshes with 19,020 (Tooth D)–28,632 (Tooth A) triangular elements of varying sizes. Mesh sensitivity tests were performed. For example, Tooth A was remeshed with triangular elements no larger than 20  $\mu\text{m}$  and an element growth rate of 1.2, for a total of 114,528 elements, quadruple the number of elements as the original model. This resulted in a 0.03% temperature difference along a representative line in the radial direction, meaning that a finer mesh had a very minor effect on the temperature elevations of the teeth. We also tested the sensitivity of the results to the time step. Each heat transfer simulation was performed with a minimum time step based on the pulse duration of the laser. Since the laser pulse is 200  $\mu\text{s}$ , we selected 100  $\mu\text{s}$  as the time step to ensure that no pulse is missed during the simulation. The time step was further decreased by half to 50  $\mu\text{s}$ , and we found that the global temperature deviation from the longer time step of 100  $\mu\text{s}$  was less than 0.08%.

A linear system solver named direct UMFPACK was used to simulate the transient heat conduction within the domain. A backward differential formula method of time stepping was chosen, and in order to accommodate the memory limitations of the computer hardware, a temperature field was saved every 0.125 s of the simulation. Each simulation was performed with these settings and using an Asus Notebook with an Intel Core 2 Duo T6400 2 GHz processor and 4 GB of RAM. Each simulation took approximately 30–50 min, with the longest time corresponding to the heat transfer simulation of Tooth A.

**Identification of Heating Protocols for Bacterial Disinfection.** The objectives of the study are to simulate temperature elevations in root dentin and its surrounding structures, and to identify realistic heating protocols that ensure delivery of sufficient thermal dosage to the deep dentin region, while preserving the surrounding tissues (i.e., periodontal ligament and bone) lining the outer root surface. To achieve an acceptable heating protocol that satisfies these requirements, the heating duration was adjusted at individual heating segments. Here, the laser heat source is traversed in the downward direction (cervical-to-apical), and then in the reverse direction (apical-to-cervical) as it moves out of the canal. The time duration at each segment is adjustable. Time increments of not less than 0.5 s were used which may be possibly controlled by the dentists, who typically hold the laser catheter during laser heating. The laser power, in this study assumed at a constant level ( $E=500$  mW) during the procedures, is not an adjustable parameter in identifying the heating protocols.

The initial heating protocol was based on previous theoretical studies [25]. Thermal damage is assumed to occur when the tissue is subject to a temperature above at least 47 °C for a minimum duration of 10 s, based on a threshold suggested by Eriksson and Albrektsson [32]. The heating duration at each segment was then adjusted to achieve the following objectives:

- (1) Maintain a temperature of at least 47 °C in the deep dentin (800  $\mu\text{m}$  measured laterally from the root canal surface), for a minimum duration of 10 s and a maximum of 11 s.
- (2) Ensure that temperatures of at least 47 °C at the root–tissue interface are maintained for less than 10 s.

Several heating protocols were conducted using the Comsol<sup>®</sup> software package, in order to determine the temperature fields in

the simulation domain. A trial-and-error approach was implemented until an adequate heating protocol, capable of satisfying the two above-stated requirements, was identified.

## Results

**Temperature Elevations in Tooth Roots.** Representative temperature contours are shown in Fig. 4 for Tooth F during the heating cycle. Results shown in this figure are based on a finalized protocol that satisfies the two design requirements. Table 2 provides the detailed values of the heat flux incident on individual root canal segments during the heating. When the laser tip is moved from the cervical segment (segment 1) to the apical segment (segment 5), the induced heat spreads laterally from the root canal surface to the deep dentin (i.e., far from the canal), limiting heat transfer in the axial direction. As the laser tip is traversed from one segment to the next, the temperature elevations in the first segment return to the original temperature of 37 °C, as shown in Fig. 4. At the same time, when the laser is moved back, in the apical-to-cervical direction, residual heat within the tooth dentin is evident. Based on the data presented, the maximum temperature occurs in the apical segment. It was found that the results obtained for the three tooth geometries were nearly identical, as expected, since the simulation procedures for the three tooth roots are very similar. Heat penetration from the root canal surface to the deep dentin of Tooth F is illustrated in Fig. 5, with the radial temperature profiles at the ends of several heating durations for three segments. Temperatures at the root canal surface vary from 70 °C (segment 2) to 95 °C (segment 5). Note that 800  $\mu\text{m}$  from the root canal surface is the assumed bacterial penetration depth. Significant temperature elevations from its baseline of 37 °C are evident at the 800  $\mu\text{m}$  location. On the contrary, the root–tissue interface locations represented by the black arrows show insufficient temperature elevations to barely 40–41 °C for segments 2 and 4. Segment 5 is close to the root apex with the thinnest root dentin, and the root–tissue interface temperature of segment 5 is elevated to more than 53 °C during the heating treatment.

One requirement for this study is that the deep dentin must maintain a temperature elevation of at least 47 °C for 10 s. Some bacteria are capable of penetrating the tubules to a distance of 800  $\mu\text{m}$  from the root canal surface. For this reason, five locations are chosen to evaluate the duration of temperature elevation in the deep dentin, 800  $\mu\text{m}$  laterally from the root canal surface, as highlighted in Fig. 6.

The transient temperature elevation in the deep dentin location for segment 2 is plotted in Fig. 7. Once the laser tip is moved to segment 2, it takes only approximately 2 s for the deep dentin location to heat up to 47 °C. Based on Fig. 7, due to the first and the second rounds of heating, the segment is elevated above 47 °C for a total of 11 s. This same procedure is followed to determine the durations of the temperature elevations in other segments of each root. Later on, this time duration is used to evaluate whether the first design requirement is satisfied.

Figure 8 provides the temperature elevations at all five deep dentin locations. All locations have two temperature peaks except the apical segment. Segment 5, at the apical site, has a total heating time of 6 s, however, the deep dentin temperature is elevated above 47 °C for more than 10 s. The residual heat accumulation within the deep dentin is evident. After the first round of heating, the temperatures at all locations decay, however, still higher than 41 °C before the second round. Temperature elevations in the second round are typically higher than that achieved in the first round.

The second requirement for the laser treatment is to ensure that no collateral thermal tissue damage occurs along the root–tissue interface, within the cementum and periodontal ligament. We assume that thermal damage occurs when the tooth–tissue interface experiences a temperature greater than 47 °C for 10 s or more. Similar to the deep dentin locations, we evaluated five

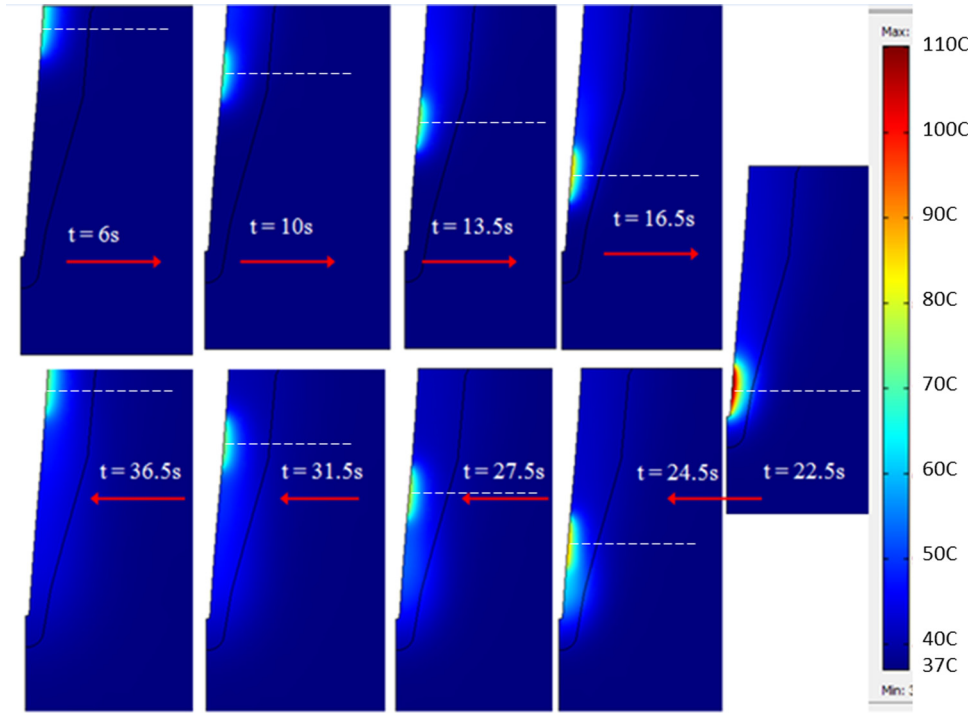


**Fig. 4 Simulated temperature contours in the dentin and surrounding tissue using the treatment protocol satisfying the two requirements for Tooth F. The white dashed lines represent the radial direction along which temperatures are plotted in Fig. 5. The black line gives the root-tissue interface.**

**Table 2 Heat flux ( $W/m^2$ ) incident on individual root canal segments at various time durations for Tooth F using the finalized heating protocol**

Time (s)	Segment 1	Segment 2	Segment 3	Segment 4	Segment 5
0–6	$1.17 \times 10^7$	0	0	0	0
6–10	0	$1.26 \times 10^7$	0	0	0
10–13.5	0	0	$1.41 \times 10^7$	0	0
13.5–16.5	0	0	0	$1.71 \times 10^7$	0
16.5–22.5	0	0	0	0	$2.42 \times 10^7$
22.5–24.5	0	0	0	$1.71 \times 10^7$	0
24.5–27.5	0	0	$1.41 \times 10^7$	0	0
27.5–31.5	0	$1.26 \times 10^7$	0	0	0
31.5–36.5	$1.17 \times 10^7$	0	0	0	0

locations along the root-tissue interface as highlighted in Fig. 6. The distance between the root-tissue interface and the deep dentin locations for segments 1–5 ranges from 110 to 1.67 mm.

The transient temperature elevations at the five interface locations are illustrated in Fig. 9. Only segment 5 of Tooth F experienced a temperature elevation greater than  $47^\circ C$ . This is expected since the distance between the root-tissue interface and the deep dentin location for segment 5 is only  $110 \mu m$ . The calculated duration when the temperature above  $47^\circ C$  is less than 9 s, therefore, the prescribed thermal damage threshold has not been reached.

**Design.** In order to satisfy the two requirements for an effective bacterial elimination, while preserving the sensitive supporting tissue structures at the root-tissue interface, we have identified suitable heating protocols for each tooth root. The adjustable parameter of the study is the heating duration at each root canal segment. We have implemented a trial-and-error approach, based on examinations of the temperature elevations in both the deep dentin

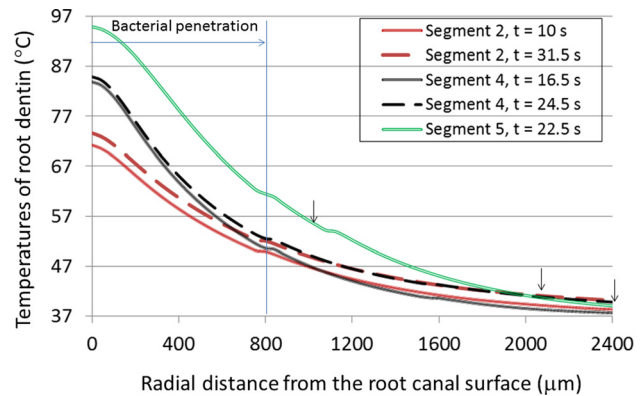


**Fig. 5 Radial temperature distributions along the white dashed lines shown in Fig. 4 at several segments. The black arrows represent the locations of the root-tissue interface. Note that  $800 \mu m$  is the assumed bacterial penetration depth from the root canal surface.**

and the outer root-tissue interface locations. Note that the method used to identify the heat protocols is not an optimization method, and more than one protocol may be identified using the trial-and-error approach, which satisfies the criteria.

Table 3 shows the progress toward the identification of a suitable heating protocol for Tooth F. In this table, two time durations are given for segments 1–4; the first value corresponds to the first round of heating, and the second value corresponds to the duration of the final round of heating. Notably, segment 5 has only one value listed because it experiences only one round of heating. No irreversible thermal damage occurs to the tooth-tissue interfaces for any of the tested protocols, shifting the primary focus to the first requirement of the protocol design, which is to elevate the deep dentin location for 10–11 s. Protocol 1F resulted in overheating at Location 2 in the deep dentin, while insufficient heating on

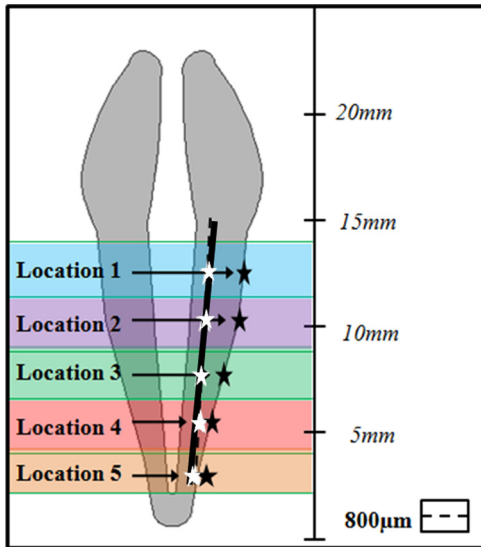


**Fig. 6 Schematic diagram of the tooth dentin and the five locations of the deep dentin (white stars) and the five locations of the root-tissue interface (black stars)**

Locations 3 and 4. Protocol 2F shows overheating at Locations 2–4. While addressing the issue at Locations 3–4 in Protocol 3F, the thermal dosage is insufficient at Location 2. Finally, protocol (Protocol 4F) is identified as being suitable because of its ability to satisfy both design requirements.

The other two teeth required similar trial-and-error adjustments of the heating times to identify suitable heating protocols. More than 15 heating protocols were tested for Tooth A and Tooth D before identifying the protocols satisfying both design requirements. The time durations of temperatures exceeding 47 °C at each of the individual locations are provided in Tables 4 and 5 for Tooth A and Tooth D, respectively. The temperature elevations in the deep dentin are maintained for between 10 and 11 s, while the temperature elevation along the tooth-tissue boundary is

minimized. Again, the most likely site for collateral thermal tissue damage to the support structure is at the apical site of the tooth, which is attributed to the comparatively low dentin thickness in this region. Fortunately, even the thinnest regions of dentin on the models are greater than 800 µm from the root canal surface. This allows for identification of an accurate heating protocol to preserve the supporting structures at the apical site, while effectively exterminating bacteria from the deep dentin. Tooth A and Tooth F have similar heating times of approximately 36.5 s, while Tooth D (the smallest) requires a much shorter heating time of 28 s.

## Discussion

Although in vitro experiments have been implemented to measure temperatures inside the root canal and the root-tissue interface during inter-canal heating using a heating catheter [33–40], a detailed understanding of the temperature distribution within the root dentin has not been available. In addition, those in vitro experiments with extracted teeth subject to room temperatures may not completely mimic the physiologic and thermal environment inside the mouth. Our results have demonstrated the potential of using a theoretical simulation to obtain a detailed description of the temperature distribution in the tooth root during bacterial disinfections by laser treatment. To our knowledge, this is also the first theoretical simulation of the temperature field in teeth based on realistic tooth root geometries of extracted human teeth. This certainly improves the predictability of heat transfer processes occurring from heating treatment in dentistry via theoretical modeling. However, like any theoretical simulations, experimental measurements are needed to validate the model. It is expected that the future experimental results will further improve the theoretical model.

There are many adjustable parameters in laser bacterial disinfection treatments. In this study, we only selected the time duration at each segment as the adjustable parameter. Since the laser catheter motion is currently controlled by the dentist who performs the procedures, an increment of 0.5 s is used in the protocol design. This definitely limits the ability to control the exact precision of the heating duration for each tooth segment. The finalized heating protocols manage to heat the deep tooth dentin above

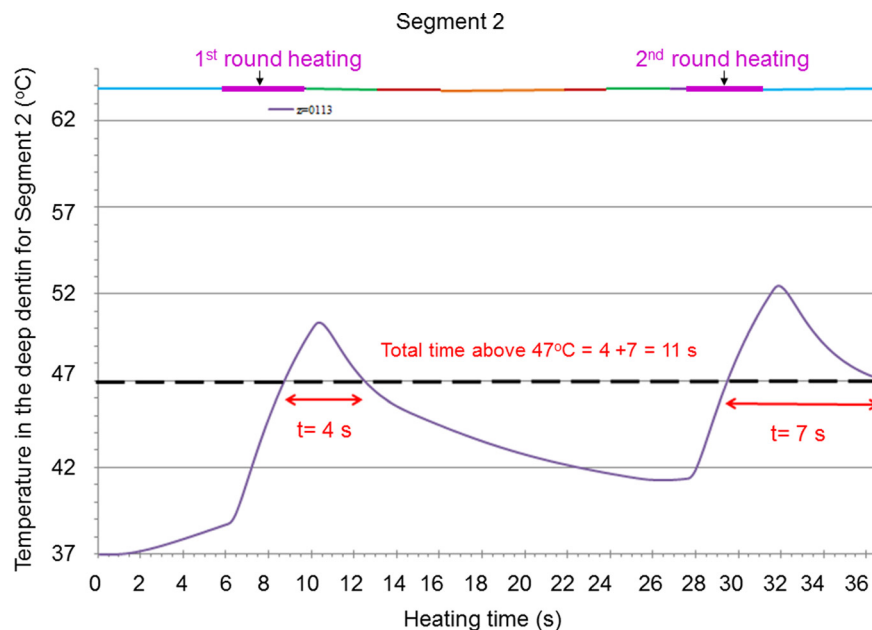


**Fig. 7 Transient temperature elevations at the deep dentin location of segment 2 of Tooth F. The bars on top of the plot give the heating duration of individual segments. The two double arrows measure the total time at the deep dentin location of segment 2 when its temperature is above 47 °C.**

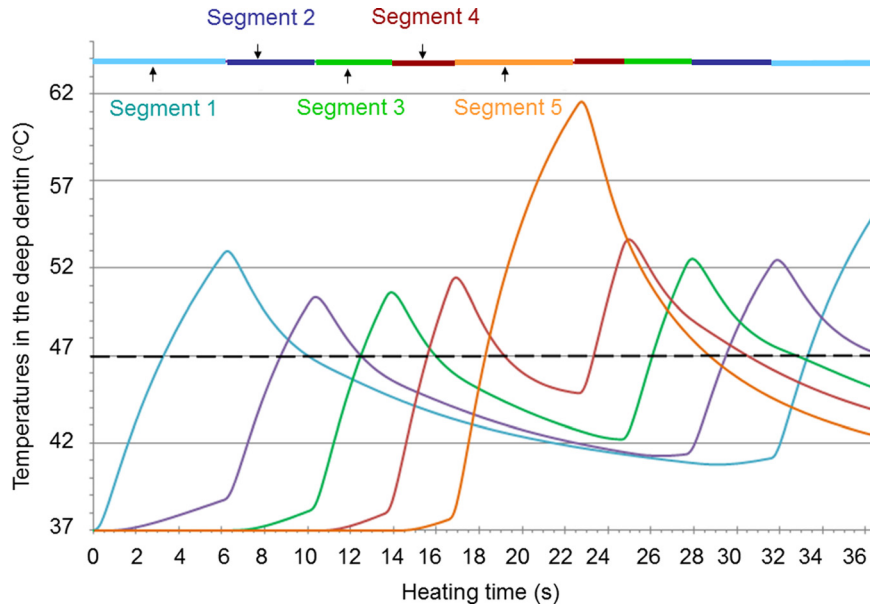


Fig. 8 Transient temperature elevations at the five deep dentin locations of Tooth F

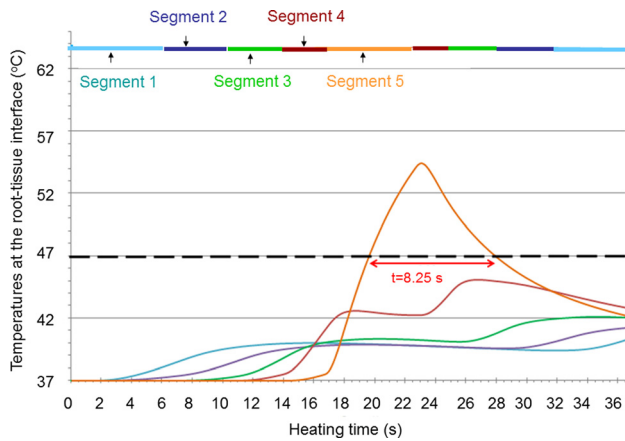


Fig. 9 Transient temperature elevations at the five locations along the root-tissue interface of Tooth F

47°C for 10–11 s. As shown in the previous heating protocols, a  $\pm 0.5$  s deviation from the proposed protocol would result in overheating or underheating for the deep dentin for more 1–1.5 s. If an apparatus were designed to control the motion of the laser throughout the treatment, the time duration when temperature is above 47°C at each deep dentin location could be precisely 10 s. Nevertheless, the current study shows the potential of using theoretical simulations to design precise heating protocols to achieve a criterion. Other parameters, such as the laser power level, can also be adjustable if a computer program is created to adjust the laser power level at individual root canal segments. This could be implemented along with a motion controlled apparatus to optimize the design for individualized laser disinfection treatments.

A depth of 800  $\mu\text{m}$  was considered, as the depth bacteria penetrated from the canal in this study, which may not always be the case. Kakoli et al. [41] demonstrated that the spreading of bacteria depends on the patient age, and that the depth of bacterial invasion decreases from 420  $\mu\text{m}$  in the young group to 360  $\mu\text{m}$  in the old group due to changes in tubule dimensions with patients' age. The differences in the penetration depth among previous experimental studies suggest that the depth of bacterial invasion is dependent on the relative sizes between the bacteria and dentin tubules, and

Table 3 Various heating protocols tested for Tooth F. The heating times represent that in the first round and the second round for segments 1–4. Segment 5 only has one round of heating.

Protocol 1F (total heating time = 38 s)					
Segments	1	2	3	4	5
Heating time (first and second rounds) (s)	6–6	4.5–4.5	3–3	2.5–2.5	6
Time when $T \geq 47^\circ\text{C}$ in deep dentin (s)	10.625	14.5	9.5	9.875	10.5
Time when $T \geq 47^\circ\text{C}$ at the interface (s)	0	0	0	0	8.25
Protocol 2F (total heating time = 39 s)					
Segments	1	2	3	4	5
Heating time (first and second rounds) (s)	6–6	4–4	3.5–3.5	3–3	6
Time when $T \geq 47^\circ\text{C}$ in deep dentin (s)	10.875	11.375	11.875	13.25	10.875
Time when $T \geq 47^\circ\text{C}$ at the interface (s)	0	0	0	0	8.625
Protocol 3F (total heating time = 37 s)					
Segments	1	2	3	4	5
Heating time (first and second rounds) (s)	6–6	4–3.5	3.5–3	3–2	6
Time when $T \geq 47^\circ\text{C}$ in deep dentin (s)	10.875	9.875	10.125	10.875	10.375
Time when $T \geq 47^\circ\text{C}$ at the interface (s)	0	0	0	0	8.25
Protocol 4F (total heating time = 36.5 s)					
Segments	1	2	3	4	5
Heating time (first and second rounds) (s)	6–5	4–4	3.5–3	3–2	6
Time when $T \geq 47^\circ\text{C}$ in deep dentin (s)	10	11	10.25	10.75	10.375
Time when $T \geq 47^\circ\text{C}$ at the interface (s)	0	0	0	0	8.25

**Table 4 Final heating protocol and time durations when  $T \geq 47^\circ\text{C}$  for Tooth A**

Segments 1-2-3-4-5-4-3-2-1		
Heating time 6.5 s–3.5 s–3.5 s–3 s–6.5 s–2.5 s–3 s–3 s–5 s		
Total heating time: 36.5 s		
Time when $T \geq 47^\circ\text{C}$ (s)		
Segments	Deep dentin locations	Root–tissue interface locations
1	10.125	0
2	10.5	0
3	10.5	0
4	10.75	0
5	10.75	0

**Table 5 Final heating protocol and time durations when  $T \geq 47^\circ\text{C}$  for Tooth D**

Segments 1-2-3-4-5-4-3-2-1		
Heating time 4.5 s–3 s–2 s–2 s–5.5 s–2.5 s–2.5 s–3 s–3 s		
Total heating time: 28 s		
Time when $T \geq 47^\circ\text{C}$ (s)		
Segments	Deep dentin locations	Root–tissue interface locations
1	10.25	0
2	10.125	0
3	10	0
4	10.625	0
5	10.625	7.5

the motility of bacteria in the fluid-filled tubules [11,12]. Nevertheless, the theoretical model has the flexibility to redesign the heating treatment protocols according to patient age and consequent differences in penetration depth.

In addition, a thermal dosage exposure of  $47^\circ\text{C}$  for more than 10 s was used as the threshold for thermal damage of both the bacteria and the surrounding tissues [32]. Very limited research has been performed on bacterial tolerance to heating and thermal damage to cementum and the periodontal ligament with temperature elevations. Bacterial cells are typically less sensitive than mammalian cells, since they are covered by resistant cell wall, and are capable of surviving as dormant cells after heat, without dying. Nevertheless, in principle, thermal damage to living organisms is a series of biochemical events of tissue cells when exposed to heat. Heat-induced tissue damage depends on heating history as described by the Arrhenius integral [42]. The Arrhenius model suggests that when the heating time is elevated  $1^\circ\text{C}$  higher, the heating time needed for inducing tissue damage can be approximately cut in half over a limited temperature range, such as  $37\text{--}50^\circ\text{C}$ . Based on similar principle, tissue damage in heating treatment can also be assessed as  $ET_{43}$ , which is defined as the equivalent heating time under  $43^\circ\text{C}$ . Figure 6 gives the temperature elevation history at one deep dentin location. The calculated  $ET_{43}$  should be much longer than the actual heating duration, since the temperature has been raised much higher than  $43^\circ\text{C}$ . Experiments can be performed to calculate  $ET_{43}$  for a specific bacterium, and then one may compare experimental results to the calculated  $ET_{43}$  to assess thermal damage based on the protocol design. Unfortunately, the  $ET_{43}$  for targeted bacteria and the coefficients needed for calculating the Arrhenius integral to bacteria in dentin, the cementum, and periodontal ligament, are presently

unavailable. Once the parameters are determined, the developed theoretical model in this study can be again modified to design the treatment protocols with a more accurate understanding of tissue damage. The combination of a thermal damage assessment using the Arrhenius integral, and an application of an optimization method could lead to the development of an optimal thermal treatment protocol for individual teeth and patients.

The theoretical simulation provides insights on how to apply the results to clinical settings. Based on our simulation, collateral thermal damage to the root–tissue interface is unlikely if bacteria do not penetrate all the way to the cementum and periodontal ligament, and the heating in the deep dentin locations is controlled. On the other hand, the design is evolved, leading to a final protocol to satisfy sufficient heating in the deep dentin. Heat spreads from the root canal surface can be affected by the laser irradiance incident on the root canal surface, as well as by the thermal properties of root dentin and heating time. The length of the tooth root plays an important role on how the heat flux is calculated. The temperature elevations in deep dentin, in theory, should be approximately proportional to the heat transferred from the root canal surface per tissue volume, based on the linear heat conduction equation and its boundary condition. Assuming similar root canal sizes, a longer tooth root requires a longer heating time. For example, the largest tooth has a root length of 17.54 mm, and the calculated heating time is 36.5 s. Since the smallest tooth has a root length of 11.67 mm, a rough calculation of the heating time is  $24.3\text{ s}$  ( $36.5 \times 11.67 / 17.54$ ), which does not deviate too much from that calculated in the protocol (26 s). In addition, for tooth root with similar geometries and sizes, the treatment time can be adjusted due to change in thermal properties as well as the bacterial penetration depth. This can be quantitatively described by the Fourier number (dimensionless time) as

$$Fo = \alpha t / L^2 \quad (4)$$

where  $\alpha$  is the thermal diffusivity of the dentin,  $t$  is the heating time, and  $L$  is the distance from the root canal wall to the targeted deep dentin location. This dimensionless time provides a general rule in heat conduction, i.e., the heating time required will be four times of the original duration if the distance is doubled. For example, depending on the tooth age, bacterial penetration to the deep dentin is smaller with an older tooth. If the bacteria only penetrated to  $400\ \mu\text{m}$  rather than  $800\ \mu\text{m}$ , the total heating time for the largest tooth should be 8.5 s, which is approximately  $1/4$  of 36.5 s. The heating time can also be adjusted, if the thermal diffusivity changes. As shown in previous studies [43] age and disease introduce changes in the structure of dentin, and may consequently induce changes important to the thermal properties of dentin. Based on Eq. (4), the heating time is inversely proportional to the thermal diffusivity. If the thermal diffusivity is doubled, i.e., becoming more thermally conductive, the heating time can be decreased by 50%. Currently, there are very limited studies to quantify thermal property of normal teeth, let alone the teeth with aging and diseases.

As with all investigations, there are limitations to this study that should be recognized. We did not model optical fluctuation and dependence of optical properties on temperature related dehydration. Also, the laser irradiation is modeled as a uniform heat flux incident on the root canal wall segment. Although this satisfies the overall energy deposited into the root dentin, the heat flux may not be uniform due to the end-firing design of the laser catheter tip and beam divergence. Note that a two-dimensional axis-symmetrical model for the root structure was used in light of computational resources and the simulation software. A three-dimensional tooth model could potentially improve the accuracy of the theoretical simulation, which would provide improved information about the temperature distribution within the dentin and surrounding tissue. The current study also used constant thermal properties for the human tissue and dentin models, however, these values may evolve as research in the field presses forward.

Although heating occurs for very short periods of time in this study, it is possible that a phase change may occur at the dentin surface, especially at the apex. Based on our simulation, the average temperatures at the root canal surface should not exceed the boiling temperature of water. However, the pulsed laser may induce high peak temperature elevations at the root canal surface during a pulse. Improved theoretical simulations considering the possible consequences of phase change in the dentin may be warranted [44].

In summary, we have developed a heat transfer model based on radiographic images of extracted human tooth roots to simulate heat spreading from the root canal surface to the deep root dentin during laser treatment. It has been demonstrated that root size and shape play an important role in determining the temperature elevations in both root dentin and surrounding tissue structures. The theoretical model allows identification of three laser treatment protocols for various root sizes, which may be applied to realistic clinical applications for individual patients.

## Acknowledgment

This study was supported by an NSF MRI Grant No. CBET-0821236 and a research grant from the University of Maryland Baltimore County (UMBC) Research Seed Fund Initiative.

## References

- [1] American Dental Association Survey Center, 2007, "Survey of Dental Services Rendered for Years 2005–2006," American Dental Association, Chicago.
- [2] Card, S. J., Sigurdsson, A., Orstavik, D., and Trope, M., 2002, "The Effectiveness of Increased Apical Enlargement in Reducing Intracanal Bacteria," *J. Endod.*, **28**, pp. 779–783.
- [3] Jha, D., Guerrero, A., Ngo, T., Helfer, A., and Hasselgren, G., 2006, "Inability of Laser and Rotary Instrumentation to Eliminate Root Canal Infection," *J. Am. Dent. Assoc.*, **137**, pp. 67–70.
- [4] Perez, F., Rochd, T., Lotter, J. P., Calas, P., and Michel, G., 2000, "In Vitro Study of the Penetration of Three Bacterial Strains Into Root Dentine," *Oral Surg., Oral Med., Oral Pathol.*, **76**(1), pp. 97–103.
- [5] Sjogren, U., Figdor, D., Persson, S., and Sundqvist, G., 1997, "Influence of Infection at the Time of Root Filling on the Outcome of Endodontic Treatment of Teeth With Apical Periodontitis," *Int. Endod. J.*, **30**, pp. 297–306.
- [6] Alley, B., Kitchens, G., Alley, L., and Eleazer, P., 2004, "A Comparison of Survival of Teeth Following Endodontic Treatment Performed by General Dentists or by Specialists," *Oral Surg. Oral Med. Oral Pathol. Oral Radiol. Endod.*, **98**(1), pp. 327–332.
- [7] Blicher, B., Baker, D., and Lin, J., 2008, "Endosseous Implants Versus Nonsurgical Root Canal Therapy: A Systematic Review of the Literature," *Gen. Dent.*, **56**(6), pp. 576–580.
- [8] De Chevigny, C., Dao, T. T., Basrani, B. R., Marquis, V., Farzaneh, M., Abitbol, S., and Friedman, S., 2008, "Treatment Outcome in Endodontics: The Toronto Study—Phase 4: Initial Treatment," *J. Endod.*, **34**(3), pp. 258–263.
- [9] Ng, Y. L., Mann, V., and Gulabivala, K., 2011, "A Prospective Study of the Factors Affecting Outcomes of Nonsurgical Root Canal Treatment: Part 1: Periapical Health," *Int. Endod. J.*, **44**(7), pp. 583–609.
- [10] Peneis, V. A., Fitzgerald, P. I., Fayad, M. I., Wenckus, C. S., BeGole, E. A., and Johnson, B. R., 2008, "Outcome of One-Visit and Two-Visit Endodontic Treatment of Necrotic Teeth With Apical Periodontitis: A Randomized Controlled Trial With One-Year Evaluation," *J. Endod.*, **34**(3), pp. 251–257.
- [11] Shovelton, D. H., 1964, "The Presence and Distribution of Micro-Organisms Within Non-Vital Teeth," *Br. Dent. J.*, **117**, pp. 101–107.
- [12] Siqueira, J. F., Jr., De Uzeda, M., and Fonseca, M. E., 1996, "A Scanning Electron Microscopic Evaluation of In Vitro Dentinal Tubules Penetration by Selected Anaerobic Bacteria," *J. Endod.*, **22**, pp. 308–310.
- [13] Drake, D. R., Wiemann, A. H., Rivera, E. M., and Walton, R. E., 1994, "Bacterial Retention in Canal Walls In Vitro: Effect of Smear Layer," *J. Endod.*, **20**, pp. 78–82.
- [14] Haapasalo, M., and Orstavik, D., 1987, "In Vitro Infection and Disinfection of Dentinal Tubules," *J. Dent. Res.*, **66**(8), pp. 1375–1379.
- [15] Love, R. M., "Enterococcus Faecalis—A Mechanism for Its Role in Endodontic Failure," *Int. Endod. J.*, **34**, pp. 399–405.
- [16] Ng, Y., Mann, V., Rahbaran, S., Lewsey, J., and Gulabivala, K., 2007, "Outcome of Primary Root Canal Treatment: A Systematic Review of the Literature—Part 1. Effects of Study Characteristics on Probability of Success," *Int. Endod. J.*, **40**, pp. 921–939.
- [17] Ng, Y., Mann, V., and Gulabivala, K., 2008, "Outcome of Secondary Root Canal Treatment: A Systematic Review of the Literature," *Int. Endod. J.*, **41**, pp. 1026–1046.
- [18] Fahey, M., Onyejekwe, O., Mason, H. L., and Mitra, K., 2008, "Precise Dental Ablation Using Ultra-Short-Pulsed 1552 nm Laser," *Int. J. Heat Mass Transfer*, **51**, pp. 5732–5739.

- [19] Gordon, W., Atabakhsh, V. A., Meza, F., Doms, A., Nissan, R., Rizoiu, I., and Stevens, R. H., 2007, "The Antimicrobial Efficacy of the Erbium, Chromium, Yttrium-Scandium-Gallium-Garnet Laser With Radial Emitting Tips on Root Canal Dentin Walls Infected With *Enterococcus Faecalis*," *J. Am. Dent. Assoc.*, **138**(7), pp. 992–1002.
- [20] Moritz, A., Jakolitsch, S., Goharkhay, K., and Schoop, U., 2000, "Morphologic Changes Correlating to Different Sensitivities of *Escherichia Coli* and *Enterococcus Faecalis* to Nd:YAG Laser Irradiation Through Dentin," *Lasers Surg. Med.*, **26**, pp. 250–261.
- [21] Ishizaki, N., Matsumoto, K., Kimura, Y., Wang, X., Kinoshita, J., Okano, S., and Jayawardena, J., 2004, "Thermographical and Morphological Studies of Er,Cr:YSGG Laser Irradiation on Root Canal Walls," *Photomed. Laser Surg.*, **22**(4), pp. 291–297.
- [22] Matsuoka, E., Jayawardena, J. A., and Matsumoto, K., 2005, "Morphological Study of the Er,Cr:YSGG Laser for Root Canal Preparation in Mandibular Incisors With Curved Root Canals," *Photomed. Laser Surg.*, **23**(5), pp. 480–484.
- [23] Radatti, D. A., Baumgartner, J. C., and Marshall, J. G., 2006, "A Comparison of the Efficacy of Er,Cr:YSGG Laser and Rotary Instrumentation in Root Canal Debridement," *J. Am. Dent. Assoc.*, **137**(9), pp. 1261–1266.
- [24] Yamazaki, R., Goya, C., Yu, D., Kimura, Y., and Matsumoto, K., 2001, "Effects of Erbium, Chromium:YSGG Laser Irradiation on Root Canal Walls: A Scanning Electron Microscopic and Thermographic Study," *J. Endod.*, **27**(1), pp. 9–12.
- [25] Zhu, L., Tolba, M., Arola, D., Salloum, M., and Meza, F., 2009, "Evaluation of Effectiveness of ER,Cr:YSGG Laser for Root Canal Disinfection: Theoretical Simulation of Temperature Elevations in Root Dentin," *ASME J. Biomech. Eng.*, **131**(7), p. 071004.
- [26] Aoki, A., Mizutani, K., Takasaki, A. A., Sasaki, K. M., Nagai, S., Schwarz, F., Yoshida, I., Eguro, T., Zeredo, J. L., and Izumi, Y., 2008, "Current Status of Clinical Laser Applications in Periodontal Therapy," *Gen. Dent.*, **56**(7), pp. 674–687.
- [27] Dederich, D. N., and Bushick, R. D., 2004, "Lasers in Dentistry: Separating Science From Hype," *J. Am. Dent. Assoc.*, **135**, pp. 204–212.
- [28] Pennes, H. H., 1948, "Analysis of Tissue and Arterial Blood Temperatures in the Resting Human Forearm," *J. Appl. Physiol.*, **253**, pp. H869–H873.
- [29] Craig, R. G., and Peyton, F. A., 1961, "Thermal Conductivity of Tooth Structure, Dental Cements, and Amalgam," *J. Dent. Res.*, **40**(3), pp. 411–418.
- [30] Diao, C., Zhu, L., and Wang, H., 2003, "Cooling and Rewarming for Brain Ischemia or Injury," *Ann. Biomed. Eng.*, **31**, pp. 346–353.
- [31] Jakubinek, M. B., and Samarasekera, C., 2006, "Elephant Ivory: A Low Thermal Conductivity, High Strength Nanocomposite," *J. Mater. Res.*, **21**, pp. 287–292.
- [32] Eriksson, A. R., and Albrektsson, T., 1983, "Temperature Threshold Levels for Heat-Induced Bone Tissue Injury: A Vital-Microscopic Study in the Rabbit," *J. Prosthet. Dent.*, **50**, pp. 101–107.
- [33] Floren, J. W., Weller, N., Pashley, D. H., and Kimbrough, W. F., 1999, "Changes in Root Surface Temperatures With In Vitro Use of the System B HeatSource," *J. Endod.*, **25**, pp. 593–595.
- [34] Jung, I. Y., Lee, S. B., Kim, E. S., Lee, C. Y., and Lee, S. J., 2003, "Effect of Different Temperatures and Penetration Depth of a System B Plugger in the Filling of Artificially Created Oval Canals," *Oral Surg. Oral Med. Oral Pathol. Oral Radiol. Endod.*, **96**, pp. 453–457.
- [35] Lipski, M., 2005, "Root Surface Temperature Rises During Root Canal Obturation, In Vitro, by the Continuous Wave of Condensation Technique Using System B HeatSource," *Oral Surg. Oral Med. Oral Pathol. Oral Radiol. Endod.*, **99**, pp. 505–510.
- [36] Lipski, M., 2006, "In Vitro Infrared Thermographic Assessment of Root Surface Temperatures Generated by High-Temperature Thermoplasticized Injectable Gutta-Percha Obturation Technique," *J. Endod.*, **32**, pp. 438–441.
- [37] Lipski, M., and Wozniak, K., 2003, "In Vitro Infrared Thermographic Assessment of Root Temperature Rises During Thermafil Retreatment Using System B," *J. Endod.*, **29**, pp. 413–415.
- [38] Romero, A. D., Green, D. B., and Wucherpfennig, A. L., 2000, "Heat Transfer to the Periodontal Ligament During Root Obturation Procedures Using an In Vitro Model," *J. Endod.*, **26**(2), pp. 85–87.
- [39] Sweetman, T. L., Baumgartner, J. C., and Sakaguchi, R. L., 2001, "Radicular Temperatures Associated With Thermoplasticized Gutta-Percha," *J. Endod.*, **27**(8), pp. 512–515.
- [40] Villegas, J. C., Yoshioka, T., Kobayashi, C., and Suda, H., 2005, "Intracanal Temperature Rise Evaluation During the Usage of the System B: Replication of Intracanal Anatomy," *Int. Endod. J.*, **38**, pp. 218–222.
- [41] Moritz, A. R., and Henriques, F. C., 1947, "The Relative Importance of Time and Surface Temperature in the Causation of Cutaneous Burns," *Am. J. Pathol.*, **23**, pp. 695–720.
- [42] Kakoli, P., Nandakumar, R., Romberg, E., Arola, D., and Fouad, A. F., 2009, "The Effect of Age on Bacterial Penetration of Radicular Dentin," *J. Endod.*, **35**(1), pp. 78–81.
- [43] Arola, D., 2007, "Fracture and Aging in Dentin," *Dental Biomaterials: Imaging, Testing and Modeling*, R. Curtis and T. Watson, eds., Woodhead Publishing, Cambridge, UK.
- [44] Abraham, J., and Sparrow, E., 2007, "A Thermal Ablation Model Including Liquid-to-Vapor Phase Change, Necrosis-Dependent Perfusion, and Moisture-Dependent Properties," *Int. J. Heat Mass Transfer*, **50**, pp. 2537–2544.